Journal of Advanced Research (2015) 6, 1031–1044

Cairo University

Journal of Advanced Research

ORIGINAL ARTICLE

Hydrogeochemical evolution of inland lakes' water: A study of major element geochemistry in the Wadi El Raiyan depression, Egypt

Essam A. Mohamed [a], Ahmed M. El-Kammar [b], Mohamed M. Yehia [c], Hend S. Abu Salem [b,*]

[a] *Geology Department, Faculty of Science, Beni Suef University, Egypt*
[b] *Geology Department, Faculty of Science, Cairo University, Egypt*
[c] *Central Laboratory for Environmental Quality Monitoring, National Water Research Centre, Kanater El-Khairia, Egypt*

ARTICLE INFO

Article history:
Received 19 July 2014
Received in revised form 14 December 2014
Accepted 25 December 2014
Available online 3 January 2015

Keywords:
Surface water
Major elements
Geochemical evolution
Faiyum
El Raiyan depression

ABSTRACT

Wadi El Raiyan is a great depression located southwest of Cairo in the Western Desert of Egypt. Lake Qarun, located north of the study area, is a closed basin with a high evaporation rate. The source of water in the lake is agricultural and municipal drainage from the El Faiyum province. In 1973, Wadi El Raiyan was connected with the agricultural wastewater drainage system of the Faiyum province and received water that exceeded the capacity of Lake Qarun. Two hydrogeological regimes have been established in the area: (i) higher cultivated land and (ii) lower Wadi El Raiyan depression lakes. The agricultural drainage water of the cultivated land has been collected in one main drain (El Wadi Drain) and directed toward the Wadi El Raiyan depression, forming two lakes at different elevations (upper and lower). In the summer of 2012, the major chemical components were studied using data from 36 stations distributed over both hydrogeological regimes in addition to one water sample collected from Bahr Youssef, the main source of freshwater for the Faiyum province. Chemical analyses were made collaboratively. The major ion geochemical evolution of the drainage water recharging the El Raiyan depression was examined. Geochemically, the Bahr Youssef sample is considered the starting point in the geochemical evolution of the studied surface water. In the cultivated area, major-ion chemistry is generally influenced by chemical weathering of rocks and minerals that are associated with anthropogenic inputs, as well as diffuse urban and/or agricultural drainage. In the depression lakes, the water chemistry generally exhibits an evaporation-dependent evolutionary trend that is further modified by cation exchange and precipitation of carbonate minerals.

* Corresponding author. Tel.: +20 1115797536.
E-mail address: hendsaeed@gmail.com (H.S. Abu Salem).

Peer review under responsibility of Cairo University.

Production and hosting by Elsevier

Introduction

The Wadi El Raiyan depression is located in the Western Desert, 40 km southwest of Faiyum Province, and has an estimated area of 703 km^2. It is situated between latitudes 28°45′ and 29°20′N and longitudes 30°15′ and 30°35′E. Since 1973,

http://dx.doi.org/10.1016/j.jare.2014.12.008
2090-1232

the depression has been used as a reservoir for agricultural drainage water. Approximately 200 million cubic meters of drainage water from cultivated lands are transported annually via El Wadi Drain to the Wadi El Raiyan lakes [1]. Two man-made lakes (i.e., upper and lower) joined by a channel were built at two different altitudes (Fig. 1). The upper lake covers an area of approximately 53 km^2 at an elevation of 10 m below sea level. The upper lake is completely filled with water and surrounded by dense vegetation [2]. The excess water of this lake flows to the lower lake via a shallow connecting channel [3]. The lower lake is larger than the upper lake and has an estimated area of approximately 110 km^2 at an elevation of 18 m below sea level [4]. The recorded maximum water depth in the lower lake is 33 m [5]. The inflow of water to the lower lake varied from 17.68×10^6 m^3 in March 1996 to 3.66×10^6 m^3 in July 1996, with a total annual inflow of 127.2×10^6 m^3/year [5]. The area between these two lakes is used for fish farming.

The major ionic composition of the surface water can reveal the type of weathering and a variety of other natural and anthropogenic processes on a hydrological basin-wide scale. Since the earlier works [6–9], the major element geochemistry of numerous major rivers has been studied, notably including the Amazon [10–13], Ganges–Brahmaputra [14–16], Lena [17–19], Makenzie [20], and Orinoco [21,22]. Studies have shown that there are a variety of processes that control the geochemical characteristics and variety of river water geochemistry. These processes include rainfall type, degree of evaporation, weathering of the bedrock, bedrock mineralogy, temperature, relief, vegetation and biological uptake.

To the authors' knowledge, there have been few published studies and insufficient data on the geochemical evolution of drainage water in the study area. Those studies include the works of Saleh [2], Sayed and Abdel-Satar [3], Saleh et al. [23,24]. This article addresses the water geochemistry of an integrated drainage system that drains through different sources of agricultural wastewater into an artificial inland depression (Figs. 1 and 2).

The area supports rich and varied desert wildlife and unique geological and geomorphological features [25]. Since 1973, the Wadi El Raiyan lakes have attracted large populations of birds, particularly waterfowl. The two lakes are currently among the most important Egyptian wetland areas and are likely to assume international importance for migrating waterfowl in the future.

The inorganic pollutants in the Wadi El Raiyan lakes were studied by Saleh et al. [23] in 2000. The study documented a significant improvement in the water quality of the Wadi El Raiyan lakes compared to 1988 as reported by Saleh et al. [24]. Mansour and Sidky [4] compared the major components of contamination between the Lake Qarun and Wadi El Raiyan wetlands, and they concluded that Lake Qarun was more polluted than the Wadi El-Raiyan lakes and that the lower lake of this wetland was relatively more contaminated than the upper lake.

Bedrock geology

El Faiyum Depression is a natural depression in the Western Desert of Egypt and extends over 12,000 km^2. Tablelands surround the Faiyum Depression on the east, west and south and separate it from neighboring depressions, the Nile Valley and Wadi El Raiyan. The Faiyum Depression is underlain by rocks of the Middle Eocene, which form the oldest exposed beds in the area and are composed essentially of gypsiferrous shale,

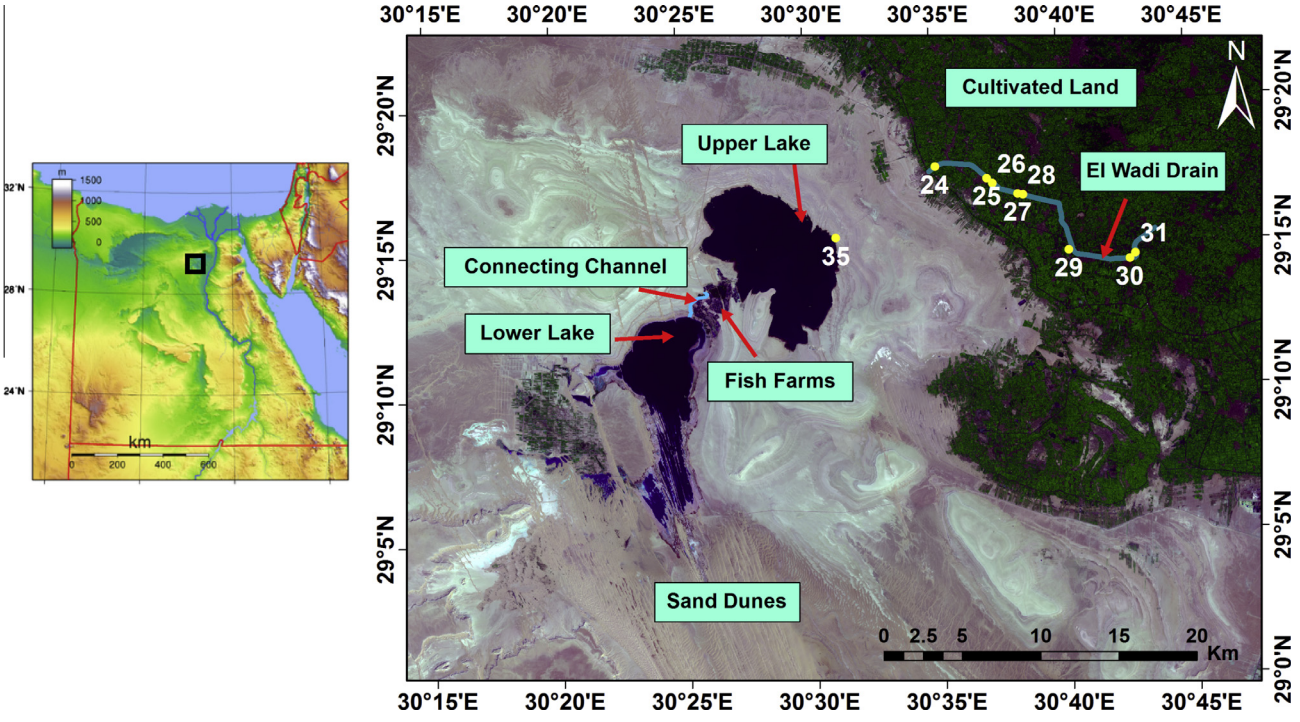

Fig. 1 Location map of the Wadi El Raiyan upper and lower lakes, El Wadi drain and location of collected water samples from the cultivated land "as shown in yellow circles".

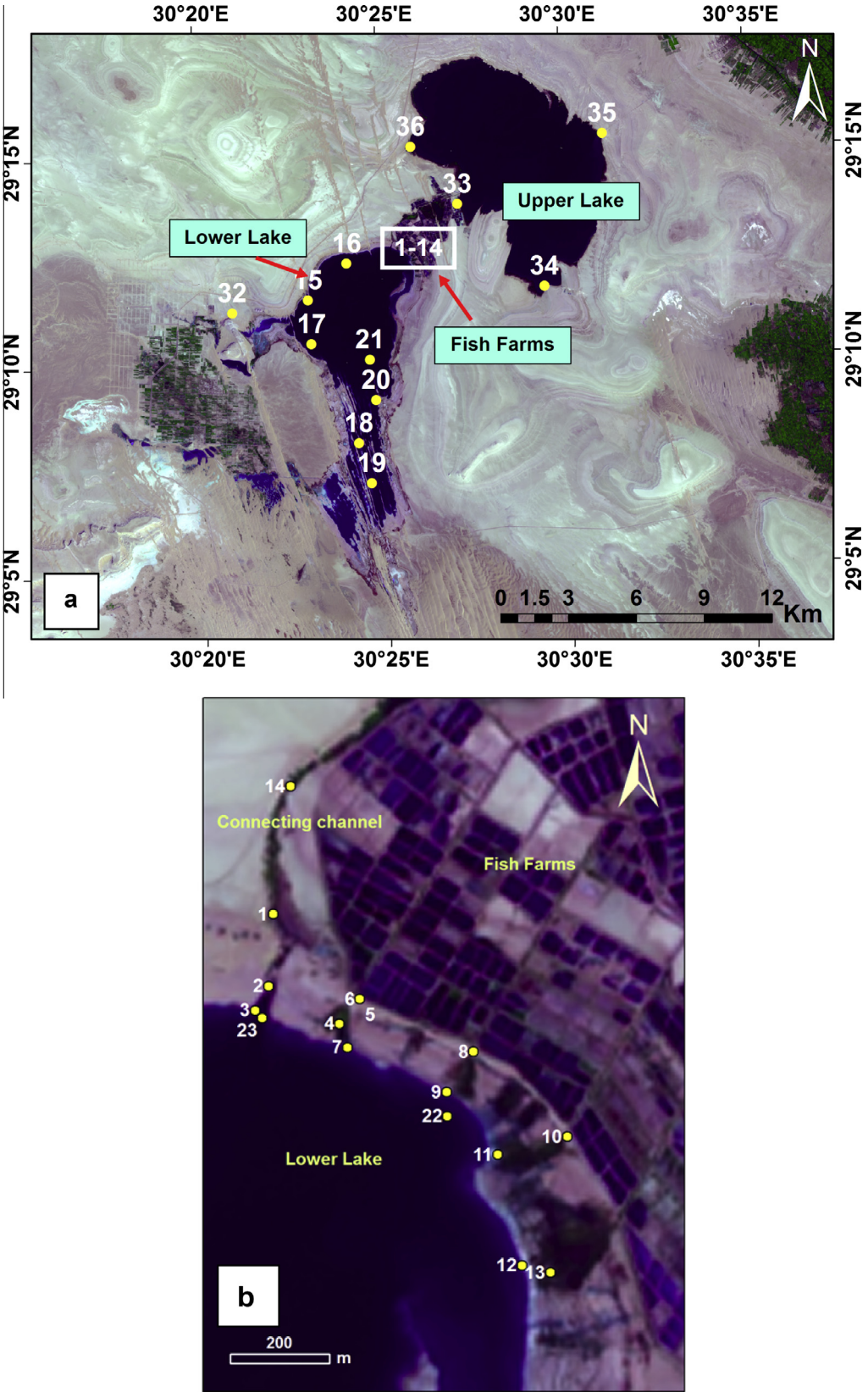

Fig. 2 (a) The location of the collected samples from upper and lower lakes and the fish farms area, (b) The fish farm samples (1–14, white box), samples 5 and 6 have the same point.

white marls, limestone and sand [26,27]. Quaternary deposits are widely distributed over the Faiyum area in the form of eolian, Nilotic and lacustrine deposits (Fig. 3).

Most of the cultivated lands in the Faiyum province are deep alluvial loam or clayey, derived mainly from Nile flood alluvium. The depression forms a more or less level plain, from which the ground slopes gently away at the northern side toward Lake Qarun and to the southwest toward the Wadi El Raiyan. It has a dense network of irrigation canals and drains. In addition, calcareous clayey and some sandy soils are found in patches toward the edge of the depression [28,29].

The Wadi El Raiyan depression was naturally formed in Middle Eocene carbonates (Fig. 3). The Middle Eocene sedimentary sequence consists of two formations, the Qaret Gehannam Formation and the underlying Wadi El Raiyan Formation. The Qaret Gehannam Formation has a thickness of approximately 50 m and consists of Nummulitic limestone in addition to shale, gypsum and marlstone intercalated with limestone. The Wadi El Raiyan Formation is located in the south of the depression and consists mainly of very hard limestone with alternating Nummulitic limestone and occasional argillaceous sandstone. The Nummulitic limestone is intercalated with reefal limestone at its base.

Methodology

In August 2012, 36 water samples were collected from the Wadi El Raiyan lakes and their recharging drain (El Wadi drain) and at fish farms that have been developed between the upper and lower lakes (Fig. 1 and Fig. 2b). The samples were placed in polyethylene bottles for laboratory analysis. Two bottles of one-liter capacity each were used for major element and biochemical oxygen demand (BOD) analyses. The samples were placed in iceboxes before being transported to the central chemical analysis laboratories of the National Water Research Centre, El-Kanater El-Khairia, Egypt.

The sampling and analytical methods were performed following British Standard Institute (BSI) water sampling

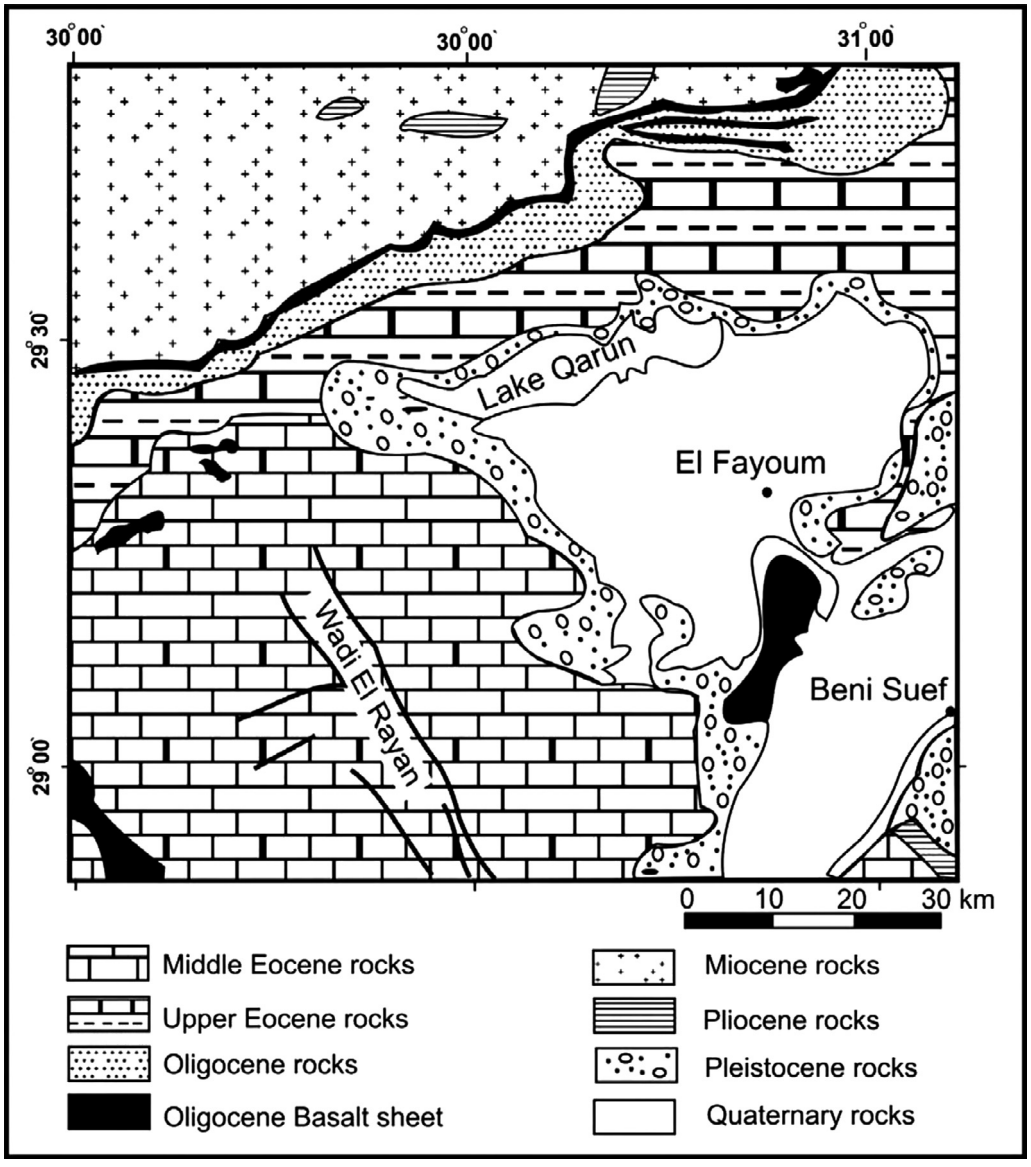

Fig. 3 Geological map of El Faiyum area [30].

and analytical methods. pH, temperature, conductivity and total salinity were measured in situ using standard field equipment. Acid-washed, airtight sample bottles were rinsed with surface water at the sampling site and then filled to the top. Total alkalinity, which is the sum of CO_3^{2-} and HCO_3^-, was measured by titration within a few hours of sampling using 0.02 N sulfuric acid with a few drops of phenolphthalein and methyl orange as indicators according to the standard method. The water samples were filtered through 0.45-μm polypropylene filter membranes before analysis.

Water samples for cation analysis were acidified to pH < 2 with ultra-pure nitric acid and kept in a refrigerator. Cations (K, Na, Mg and Ca) were analyzed using an 11355 Inductively Coupled Plasma (ICP) Multi Element Standard + 0.2% (Merck reference) with concentration 1000 mg + 10/L, and an arsenic standard solution (As = 99 + 5 mg/L Merck) was used as a standard for measurement. Anions (Cl, SO_4, and NO_3) were measured by ion chromatography (IC) using a model DX-500 chromatograph system with a CD20 Conductivity Detector. To check the quality of the overall analytical data, all of the surface water geochemical data obtained in this study were assessed for charge balance using Geochemist Workbench. Under this scheme, water analyses with a charge balance of greater than ±5% should be rejected from the data set. In this study, all of the samples met the recommended balance. This is because of the replication of each sample; each replicate was analyzed three times and the average of the six measurements for each element was taken. The activity of ions, minerals speciation and saturation indices were calculated using PHREEQC software [31]. The chemical analyses of water samples were plotted on a diagram developed by Chadha [32] to identify the different water types, and on Gibbs diagram [33,34] to investigate the natural mechanisms, which control the water chemistry.

Results

Water acidity and total dissolved solid (TDS) distribution

The water samples are mainly alkaline, with pH values in the range of 7.5–8.9 (Table 1). The drain water samples from the cultivated land have relatively lower pH values, ranging from 7.5 to 8.1. The pH increases to 8.9 in the recharge water to the upper lake from El Wadi Drain (sample 35). The upper lake shows the highest pH values except sample number 35 (Fig. 1), which is related closely to El Wadi Drain. The pH values of the water samples from the fish farms range from 7.7 to 8.2 but increase to 8.6 in the lower lake (Table 1).

The total dissolved solids (TDS) are lowest in the water samples from El Wadi Drain (Table 1) but increase in the lower lake water. The average TDS in the drainage water from cultivated land is 718 mg/l. However, TDS increases to 2658 mg/l in the upper lake waters and 2504 mg/l in the fish farm samples. The highest value of TDS (14,963 mg/l) was obtained from lower lake samples. The TDS values of the samples collected from the upper lake fall between the cultivated land and the fish farm values (Table 1), except for sample number 32 (Fig. 2a). This sample was collected from the western side of the study area (Fig. 2a); it is pumped from the upper lake through pipelines to irrigate a wide reclaimed area in the west of the lower lake and represents the drainage water of this area. The pH values are directly proportional to the TDS concentrations (Table 1).

Major element geochemistry

The concentrations of the major elements, including K, Na, Mg, Ca, Cl and SO_4, reflect that of TDS because they tend to increase in the direction of flow (Table 1). Accordingly, the water samples from the lower lake (the last destination) represent the highest concentration of major elements and TDS than the other occurrences. Sample number 32 has higher chloride and sulfate concentrations than the rest of the upper lake samples (Table 1).

Bicarbonate concentrations do not show the same trend relative to other geochemical parameters (Table 1). The fish farms' waters have the highest average bicarbonate concentration, followed by the lower lake waters, the cultivated land drains and finally the upper lake water (Table 1).

Geochemical composition and water types

Water Type 1 (T1); (Ca–Mg–HCO_3)

The irrigation water from Bahr Youssef falls in the upper right quadrant of the Chadha diagram (type 1) (Fig. 4a). This water is fresh with a TDS of 269 mg/l and pH of 7.8. It is characterized by higher concentrations of weak acidic anions (HCO_3) relative to strong acidic anions (Cl + SO_4) and with higher concentrations of alkali earth elements (Ca + Mg) relative to alkali elements (Na + K).

Water Type 2 (T2); (Na–Cl–SO_4)

Water type 2 represents drainage water samples from cultivated lands, the upper lake, fish farms and lower lake (Fig. 4a). All type T2 water samples are characterized by higher concentrations of strong acidic anions relative to weak acidic anions and higher concentrations of alkali elements relative to alkali earth elements.

Geochemical classification

Application of the Gibbs diagrams to the water samples from the study area shows distinctive chemical variations between the water samples collected from the area (Fig. 5). The River Nile water as represented by the Bahr Youssef sample is chemically controlled by leaching of the bedrock. This process of water–rock interaction has resulted in an increased concentration of Ca and HCO_3 (Fig. 5). The drainage water from cultivated lands has an average TDS concentration higher than that of the River Nile water. Elevated TDS is associated with the increase in Cl and Na concentrations. The chemical composition of the agricultural drainage water apparently is controlled by the reaction with the bedrock with a small amount of evaporation (Fig. 5). Going further, the drain water in the upper lake, fish farms and lower lake show a gradual increase in TDS, Na and Cl concentrations. This maximizes the effect of the evaporation process on the chemical composition of the surface waters under consideration (Fig. 5).

Table 1 Physical properties and ionic concentrations of the collected water samples.

Location	Sample No.	Temperature (°C)	pH	TDS (mg/l)	EC (mmhos/cm)	Total Alkalinity (mg/l)	BOD (mg/l)	K (mg/l)	Na (mg/l)	Mg (mg/l)	Ca (mg/l)	NO_3 (mg/l)	Cl (mg/l)	SO_4 (mg/l)	CO_3 (mg/l)	HCO_3 (mg/l)
Fish Farms	1	27.7	7.7	2310.0	3.6	273.0	12.0	27.0	400.0	86.0	183.3	2.6	610.0	500.0	0.0	380.0
	2	28.0	8.2	2304.0	3.6	301.6	10.0	27.0	450.0	90.0	155.7	4.8	647.2	485.0	9.6	392.0
	4	28.4	8.1	2406.0	3.8	297.0	40.0	29.0	525.0	84.4	142.6	7.1	736.0	470.0	0.0	377.0
	5	28.5	7.9	2387.0	3.7	312.0	16.0	28.0	515.0	79.9	151.0	8.7	704.0	490.0	0.0	400.0
	6	28.8	8.2	2444.0	3.8	263.0	12.0	26.0	525.0	86.2	157.0	7.6	691.0	580.0	0.0	420.0
	8	29.3	7.8	2771.0	4.3	246.0	23.0	28.0	625.0	76.7	182.4	8.0	800.0	752.0	0.0	246.0
	10	29.1	8.3	2348.0	3.7	273.0	13.0	29.0	500.0	82.5	121.0	4.6	614.0	551.0	0.0	373.0
	11	31.8	7.7	2700.0	44.2	331.0	10.0	31.0	725.0	42.4	151.7	5.4	900.0	700.0	0.0	231.0
	13	32.7	8.0	3078.0	4.8	263.0	6.0	29.0	820.0	47.2	170.0	13.6	1020.0	731.0	0.0	263.0
	14	30.2	7.8	2291.0	3.6	302.0	11.0	27.0	470.0	75.0	130.0	2.3	602.0	550.0	0.0	300.0
	Average	29.5	8.0	2503.9	7.9	286.2	15.3	28.1	555.5	75.0	154.5	6.5	732.4	580.9		338.2
Lower Lake	3	30.4	8.5	10912.0	17.1	247.0	20.0	96.0	2700.0	189.2	505.7	< 0.2	4100.0	1500.0	52.0	295.0
	7	31.4	8.5	12083.0	18.9	301.0	8.0	100.0	2900.0	169.5	600.0	< 0.2	4300.0	1800.0	33.0	278.0
	9	31.1	8.3	14208.0	22.2	226.0	10.0	114.0	3400.0	243.4	849.4	0.0	5250.0	2200.0	43.0	226.0
	12	32.7	8.4	11782.0	18.4	219.0	5.0	104.0	2850.0	192.2	583.2	0.4	4350.0	1720.0	39.0	359.0
	15	29.8	8.4	16512.0	25.8	367.0	6.0	165.0	4100.0	400.0	350.0	0.6	6000.0	2500.0	43.0	324.0
	16	29.0	8.3	16384.0	25.6	353.0	5.0	155.0	4200.0	419.6	367.0	0.6	6200.0	2550.0	48.0	305.0
	17	30.3	8.6	16512.0	25.8	273.0	6.0	160.0	4300.0	426.0	370.0	0.6	6400.0	2600.0	49.0	224.0
	18	29.9	8.6	16896.0	26.4	353.0	6.0	165.0	4450.0	437.0	392.0	0.7	6550.0	2770.0	68.0	285.0
	19	29.9	8.6	16960.0	26.5	308.0	7.0	155.0	4500.0	434.6	382.8	0.8	6600.0	2800.0	49.0	259.0
	20	30.7	8.6	16576.0	25.9	273.0	6.0	165.0	4350.0	415.0	340.8	0.7	6400.0	2750.0	44.0	229.0
	21	30.6	8.6	16512.0	25.8	264.0	8.0	165.0	4200.0	468.0	332.8	0.8	6350.0	2870.0	73.0	191.0
	22	28.6	8.5	15616.0	24.4	291.0	7.0	150.0	3900.0	430.3	324.0	0.9	5850.0	2750.0	43.0	248.0
	23	28.9	8.6	13568.0	21.2	259.0	7.0	130.0	3580.0	400.0	290.0	0.5	5500.0	2400.0	45.0	214.0
	Average	30.3	8.5	14963.2	23.4	287.2	7.8	140.3	3802.3	355.7	437.5	0.6	5680.8	2400.8	48.4	264.4
Cultivated Land	24	29.3	7.6	638.0	1.0	200.0	10.0	9.0	125.0	20.0	50.0	6.5	150.0	110.0	0.0	200.0
	25	29.4	7.6	657.0	1.0	220.0	13.0	9.0	135.0	24.8	51.8	8.6	160.0	125.0	0.0	220.0
	26	29.5	8.1	763.0	1.2	235.0	10.0	10.0	155.0	30.0	52.7	7.6	180.0	145.0	0.0	235.0
	27	29.6	7.7	659.0	1.0	217.0	11.0	9.0	140.0	22.0	50.0	7.6	160.0	120.0	0.0	217.0
	28	29.6	7.7	658.0	1.0	214.0	12.0	10.0	140.0	21.0	49.1	7.8	162.0	121.0	0.0	214.0
	29	28.4	7.8	838.0	1.3	245.0	10.0	12.0	162.0	32.0	60.0	9.5	200.0	155.0	0.0	245.0
	30	29.2	7.7	605.0	0.9	210.0	12.0	9.0	128.0	21.0	52.0	6.8	145.0	120.0	0.0	210.0
	31	30.0	7.5	922.0	1.4	285.0	14.0	11.0	195.0	28.4	63.5	10.6	230.0	140.0	0.0	285.0
	Average	29.4	7.7	717.5	1.1	228.3	11.5	9.9	147.5	24.9	53.6	8.1	173.4	129.5	0.0	228.3
Upper Lake	32	27.2	8.0	7283.0	11.4	244.0	3.0	33.0	2000.0	185.0	420.0	12.8	2800.0	2000.0	0.0	244.0
	33	29.7	8.8	1796.0	2.8	203.0	8.0	21.0	430.0	60.8	120.3	< 0.2	580.0	500.0	33.0	170.0
	34	32.4	8.9	1783.0	2.8	198.0	3.0	16.0	400.0	59.0	121.0	< 0.2	550.0	475.0	33.0	165.0
	35	27.6	7.7	640.0	1.0	219.0	6.0	7.0	140.0	25.0	45.0	4.5	160.0	130.0	0.0	210.0
	36	30.0	8.9	1788.0	2.8	218.0	5.0	16.0	400.0	55.3	118.9	< 0.2	560.0	400.0	28.0	190.0
	Average	29.4	8.5	2658.0	4.2	216.4	5.0	18.6	674.0	77.0	165.0	8.7	930.0	701.0	18.8	195.8
Bahr Youssef	37	30.0	7.8	268.5	0.4	137.6	1.8	5.3	30.5	9.6	27.4	5.6	24.1	33.3	0.0	137.6

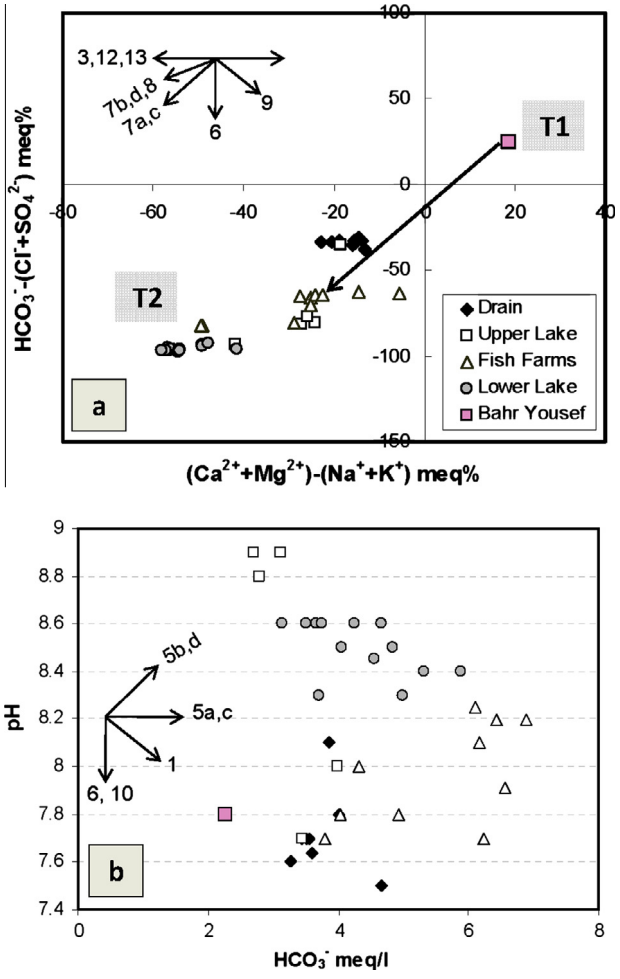

Fig. 4 (a) $(CO_3 + HCO_3)$-$(Cl + SO_4)$ versus $(Ca + Mg) + (-Na + K)$ diagram, letters in squares represent the different geochemical fields [32], (b) Variation of HCO_3 and pH in the studied water samples.

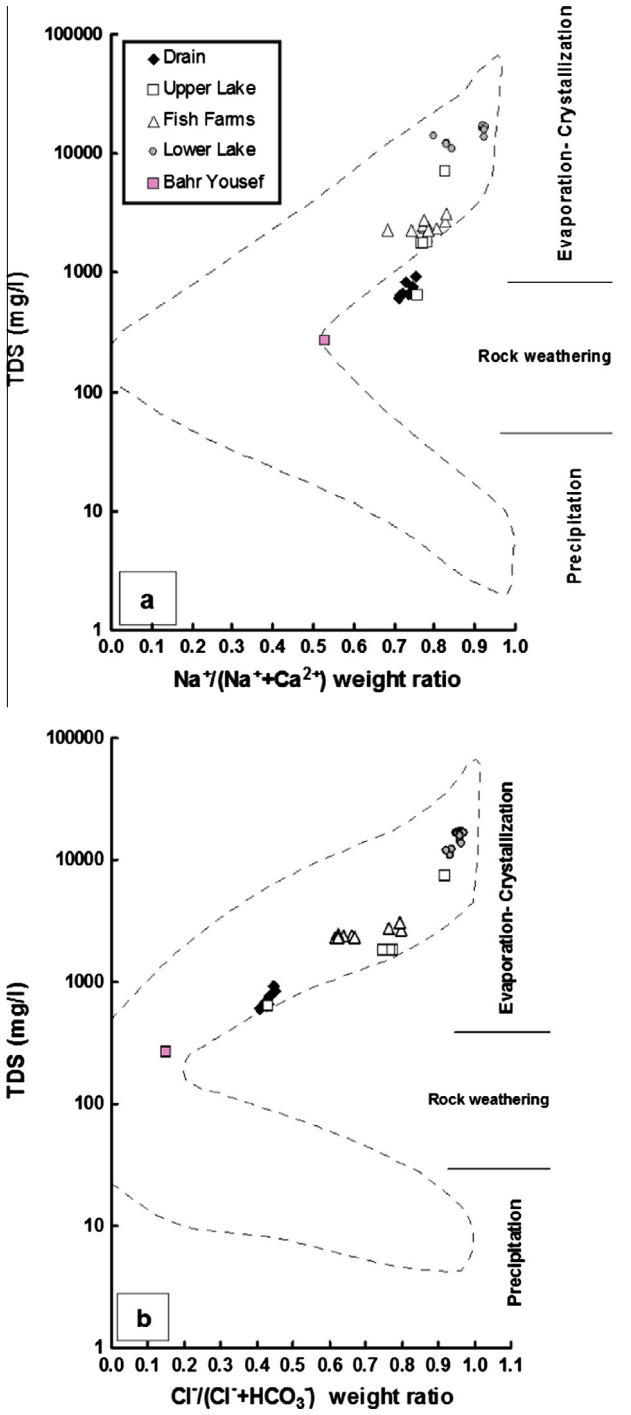

Fig. 5 Gibbs diagram for the studied water samples, (a) for cations and (b) for anions.

Discussion

The geochemistry of surface water constituents

Geochemical reactions 1–13 (Table 2) have been derived to assist in the interpretation of the geochemical reactions that control the surface water geochemistry in the area. Crossplots of all geochemical reactions that could possibly influence water chemistry were made. On the crossplots, reactions are represented by vectors according to their effect on the *X*- or *Y*-axes. If a reaction does not influence either the *X*- or *Y*-axis, it cannot be plotted on the crossplot, while if it only influences one axis or the other the vector is parallel to that axis. On the other hand, if a reaction influences both *X*- and *Y*-axis parameters, then the vector has a gradient specific to the particular reaction. Accordingly, the vector diagrams in Figs. 4, 6 and 7 help reveal the dominant geochemical reactions in the study surface waters.

The downstream progressive change of any chemical component will be a consequence of the increasing impact of geochemical processes on waters along the flow path.

Controls on chloride concentration

The chloride concentration in the water samples from the cultivated land is sevenfold greater than that in the Bahr Youssef sample. The upper lake and fish farm waters have Cl concentrations greater by fivefold and fourfold than the cultivated land, respectively. This value rises to about sixfold in the lower lake than in the upper lake waters.

Table 2 The suggested geochemical reactions to interpret the evolution of the surface water geochemistry in the study area.

Process	Geochemical reaction	Reaction
Biological processes and atmospheric gas	$CO_2 + H_2O = H_2CO_3 = H^+ + HCO_3^-$	1
Oxidation of organic matter	$O_{2(g)} + CH_2O = CO_{2(g)} + H_2O$	2
Cation exchange	$2(Na)\text{-}X + Ca^{2+} = Ca\text{-}X + 2Na^+$	3a
	$2(Na)\text{-}X + Mg^{2+} = Mg\text{-}X + 2Na^+$	3b
	$2(K)\text{-}X + Ca^{2+} = Mg\text{-}X + 2K^+$	3c
	$2(K)\text{-}X + Mg^{2+} = Mg\text{-}X + 2K^+$	3d
Na^+ and K^+ exchange by Ca^{2+} and Mg^{2+}	$(Ca)\text{-}Ex + 2Na^+_{(aq)} = Ca^{2+}_{(aq)} + (2Na)\text{-}Ex$	4a
	$(Mg)\text{-}Ex + 2Na^+_{(aq)} = Mg^{2+}_{(aq)} + (2Na)\text{-}Ex$	4b
	$(Ca)\text{-}Ex + 2K^+_{(aq)} = Ca^{2+}_{(aq)} + (2K)\text{-}Ex$	4c
	$(Mg)\text{-}Ex + 2K^+_{(aq)} = Mg^{2+}_{(aq)} + (2K)\text{-}Ex$	4d
Carbonate dissolution	$CaCO_3 + H_2CO_3 = Ca^{2+} + 2HCO_3^-$	5a
	$CaCO_3 + H^+ = Ca^{2+} + HCO_3^-$	5b
	$CaMg(CO_3)_2 + 2H_2CO_3 = Ca^{2+} + Mg^{2+} + 4HCO_3^-$	5c
	$CaMg(CO_3)_2 + 2H^+ = Ca^{2+} + Mg^{2+} + 2HCO_3^-$	5d
Iron sulfide oxidation	$\frac{15}{4}O_2 + FeS_2(s) + \frac{7}{2}H_2O = Fe(OH)_3(s) + 2SO_4^{2-} + 4H^+$	6
Carbonate precipitation	$Ca^{2+} + 2HCO_3^- = CaCO_3 + H_2O$	7a
	$Ca^{2+} + HCO_3^- = CaCO_3 + H^+$	7b
	$Ca^{2+} + Mg^{2+} + 4HCO_3^- = CaMg(CO_3)_2 + 2H_2O$	7c
	$Ca^{2+} + Mg^{2+} + 2HCO_3^- = CaMg(CO_3)_2 + 2H^+$	7d
Halite dissolution	$NaCl = Na^+ + Cl^-$	8
Dissolution of gypsum	$CaSO_4.2H_2O = Ca^{2+}_{(aq)} + SO^{2-}_{4(aq)} + 2H_2O$	9
Nitrification	$O_2 + \frac{1}{2}NH_4^+ = \frac{1}{2}NO_3^- + H^+ + \frac{1}{2}H_2O$	10
Cation exchange between Ca and Mg	$Ca\text{-}Ex + Mg^{2+} = Mg\text{-}Ex + Ca^{2+}$	11
Dissolution of albite	$2NaAlSi_3O_8 + 2H^+ = 9H_2O = Al_2Si_2O_5(OH)_4 + 2Na^+ + 4H_4SiO_4$	12
Muscovite dissolution	$2\,K(Si_3Al)Al_2O_{10}(OH)_2 + 2H^+ + 3H_2O = 3Al_2Si_2O_5(OH)_4 + 2\,K^+$	13

In arid climates, chloride in water samples has a number of sources including primary rainwater (“cyclic salts” evaporated in the soil and vadose zones during overland flow and from the rivers), dissolution of halite from sedimentary bedrock, pollution from domestic and industrial sources and road gritting [35]. The Quaternary and Eocene deposits in the area are characterized by the presence of evaporite deposits. The dissolution of halite is clearly indicated through the direct relationship between Cl and Na (Fig. 7a).

The Gibbs plot (Fig. 5b) shows a steady increase in the Cl concentration from the freshwater source (Bahr Youssef) toward the lower lake. This is associated with an increase in the Na concentration that moves toward higher Na/(Na + Ca) ratio, rather than what is expected if extreme evaporation was the main factor controlling the cation ratio, especially in the samples collected from Bahr Youssef, the cultivated land drainage and sample No. 32 from the upper lake waters (the samples plotted outside the dashed zone on the Gibbs plot). This means that cation exchange (reactions 3a and b in Fig. 7a) is responsible for the slight increase in Na concentration over that expected from halite dissolution (samples plotted above the 1:1 line in Fig. 7a). In addition, the increase of the non-chloride Na and K at the expense of Ca and/or Mg or HCO_3 in the samples from the upper lake, fish farms and lower lake (Fig. 7d and e) could be associated with clay mineral dissolution (reactions 12 and 13) releasing some Na and K ions unrelated to Cl. Another source of K could be potassium sulfate fertilizers.

Chloride can be an important source of pollution for many rivers [35]. Berner and Berner [36] estimated that approximately 30% of Cl in river water arises from pollution. Domestic sewage contains considerable Cl due to the consumption of table salts by humans. Chlorination of public water supplies for purification adds significant Cl to the Cl concentration of water. Other sources of Cl include fertilizers.

By assuming that chloride is conservative (not involved in geochemical reactions with the soil or bedrock) and because of salt recycling [36], it can be shown that evaporation together with the dissolution of halite, which is available in the bedrock lithology (reaction 8, Table 2), are the most effective controls of the evolution of Cl concentration in the surface waters of the study area. The surrounding area is represented by agricultural lands and rural communities. The latter is characterized by the absence of closed sewage networks, where the sewage is completely drained through septic tanks that possibly leak sewage water to irrigation or drainage surface water channels. The drainage of cultivated lands and the domestic use of chlorinated water are among the parameters that represent the basic sources of Cl in the drainage water of the studied area.

Due to the scarcity of the mineral sylvite in evaporites, as it deposited in very restricted conditions, dissolution of sylvite as another source of Cl cannot be expected (Fig. 7b). In addition,

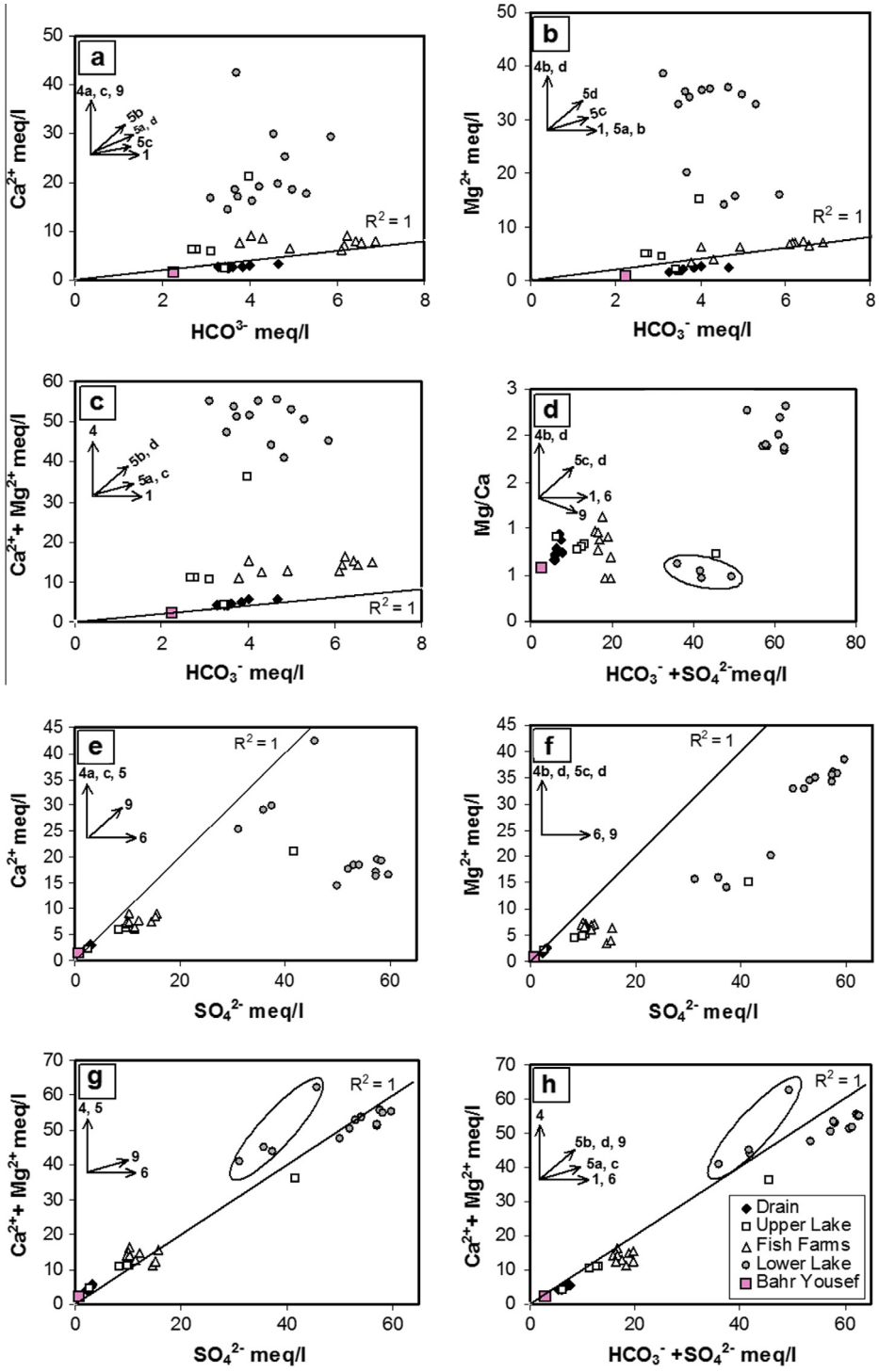

Fig. 6 Relationships between different ratios and ionic concentrations versus bicarbonate and sulfate concentrations.

cation exchange and clay minerals dissolution control the concentrations of Na and K ions in the surface waters under study.

Alkalinity and carbonate mineral reactions

Bicarbonate has a number of sources in surface water including rain, dissolution and dissociation of biogenic soil gas (reaction 1, Table 2) and dissolution of carbonate minerals (reaction 5, Table 2).

The pH of most natural waters is controlled by reactions involving the carbonate system. To obtain a pH above 7, it is necessary to introduce cations other than H^+ [37]. All water samples collected from the area are alkaline, with pH values above 7 (Table 1). The main anionic concentration in the freshwater (Bahr Youssef) is HCO_3. In the cultivated land drainage,

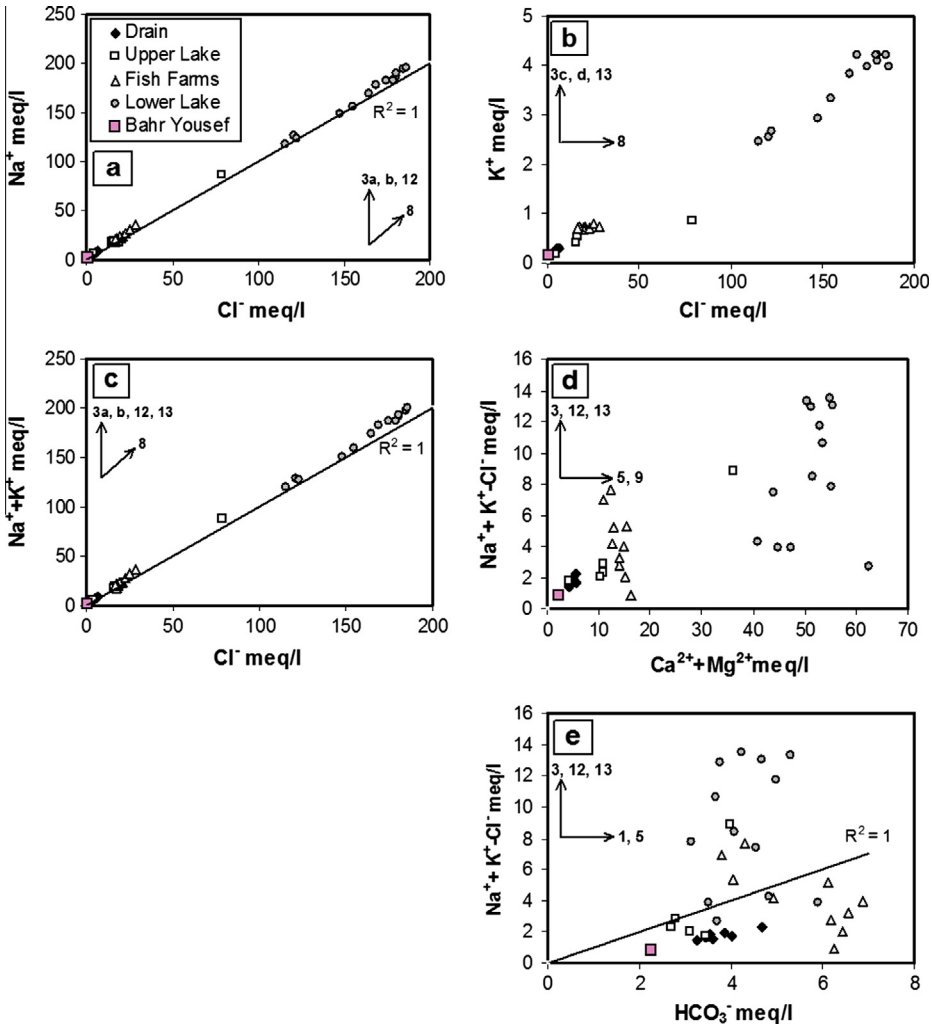

Fig. 7 Relationships between different ionic concentrations versus bicarbonate and chloride concentrations.

TDS and HCO_3 concentrations increase (Fig. 4b). Conversely, the pH is not significantly correlated with HCO_3 (Fig. 4b) and is slightly lower than that of Bahr Youssef. This can be interpreted as a result of dissolution of atmospheric CO_2 and nitrification (reaction numbers 1 and 10, respectively, Table 2). As the system is completely open, there is a continuous influx of CO_2 into the water from the atmosphere, biological processes in the soil, and via the oxidation of dead organic matter (reaction 2, Table 2). The high concentration of NO_3 in the water samples in the drains from cultivated land means that the nitrification process has been active due to contamination from the decay of plant remains, thereby increasing the acidity of the water. The increase of m_{H+} in the water has been buffered by the increase in HCO_3 concentration due to complete dissolution of carbonate minerals (reactions 5a, c, Table 2 and Fig. 4b). In the lakes, pH increases as the TDS increases (Table 1) due to the dissolution of carbonate minerals, accompanied by the reduction of pH. Therefore, besides the complete carbonate dissolution reactions (reactions 5a, c), reactions 5b, d also prevail, as they require an acid environment (Fig. 4 and Table 2).

The water in Bahr Youssef is undersaturated with respect to carbonate minerals, calcite and dolomite (Fig. 8). A saturation state has been achieved in the cultivated land drains, suggesting dissolution of carbonate minerals (i.e., the Ca, Mg and HCO_3 concentrations increase). At the same time, the dissolution of evaporites, especially gypsum, increases the concentration of Ca that drives up the saturation state of carbonate minerals, leading to their precipitation. The decrease in Ca and Mg concentrations due to the precipitation of carbonate minerals causes the Na/Na + Ca ratio to shift to the right (Fig. 5a) and below the 1:1 equivalent line with HCO_3 (Fig. 6a and b).

In the depression lakes (upper and lower lakes), the increase in TDS is accompanied by an increase in the concentration of Ca, Mg and SO_4. With continuous sources of HCO_3, the saturated state of calcite and dolomite is driven up, leading to their precipitation. As a result of calcite precipitation in the early stage of evaporation process [37], Ca is removed from the system. Accordingly, Mg concentration increases on account of Ca until the saturation of dolomite has been achieved (Fig. 8).

In the lower lake, evaporation with a continuous dissolution of evaporite may concentrate SO_4, Cl and Na. The continuous precipitation of carbonate minerals (Fig. 8) decreases the concentration of HCO_3 as well as Ca and Mg (Figs. 4 and 5), and thus cation exchange processes compensate the decrease in Ca and Mg concentrations (reaction 4, Fig. 6a–f).

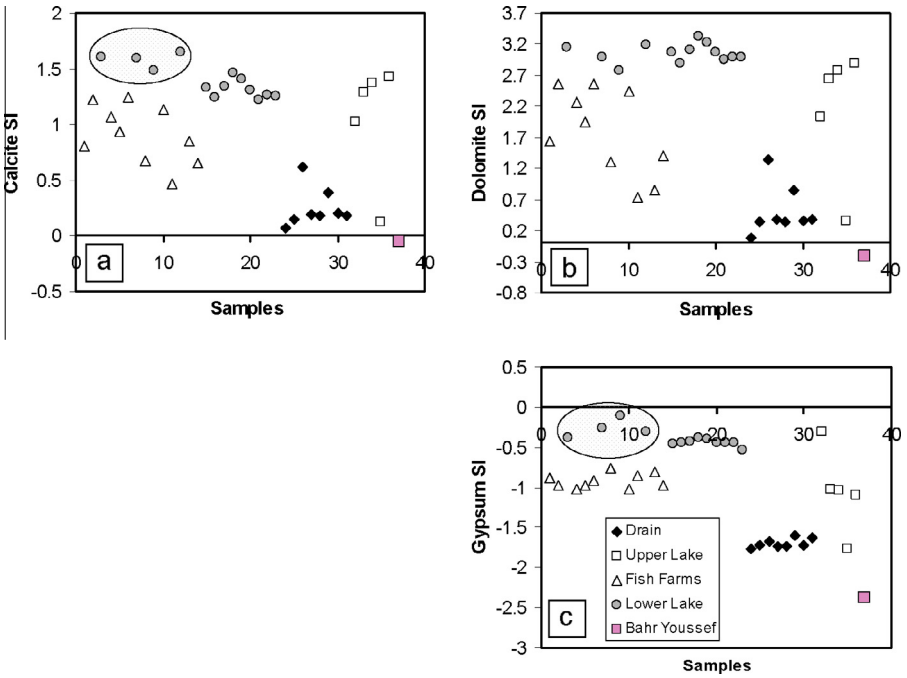

Fig. 8 Saturation indices of calcite, dolomite and gypsum for the collected water samples.

Possible sources of sulfate

Potential sources of elevated sulfate in surface water include gypsum dissolution (reaction 9), pyrite oxidation (reaction 6) and anthropogenic pollution. It is possible that a significant percentage of sulfates in surface water is from pollution sources, including burning of sulfur-rich fossil fuels, direct industrial discharge, treated sewage release and K-sulfate fertilizers [38,36].

Sulfate equivalent concentration in the irrigation water (Bahr Youssef) is 0.7 and increases to an average of 27.5 in the drainage water from cultivated land. There is a significant correlation between Ca and SO_4 in these waters ($R^2 = 0.9$) in the direction of reaction 9, dissolution of evaporites (Fig. 6e). However, pyrite oxidation should be ruled out as being responsible for increased SO_4 (reaction 6) because there is no increase in SO_4 concentration more than expected from evaporite dissolution (Fig. 6). If the sulfate came from pollution, it would be necessary to invoke a similar pollution source of calcium. This would be difficult to explain because calcium is not normally a consequence of pollution [36]. This seems to suggest that evaporite dissolution mainly controls the SO_4 concentration in the drain water. Such an increase is supported by the increase of Na and Cl [38] that is reflected in the increase of TDS from 269 in Bahr Youssef to 717 mg/l in the cultivated land drainage water.

The dissolution of gypsum from the soil of the cultivated land and the use of superphosphate fertilizers enhances the concentration of Ca in the drainage water. Therefore, the saturation indices of the carbonate minerals (calcite and dolomite) have been increased in the cultivated land drainage as well as the saturation index of gypsum; however, the water is still undersaturated with respect to gypsum (Fig. 8). The concentration of magnesium is apparently controlled by the dissolution of carbonate minerals rather than dissolution of evaporite (Fig. 6f–h).

In the Wadi El Raiyan lakes (upper and lower lakes), the equivalent concentrations of SO_4 increase from 14.6 to approximately 50 meq/l in the upper lake and lower lake, respectively. The anionic composition is in the order $Cl > SO_4 > HCO_3$, which means that the increase in the TDS resulted in the increase of SO_4 over HCO_3. In the waters of the upper lake and fish farms (Fig. 6e), there is an increase of SO_4 over that expected from gypsum dissolution. This means that other processes, possibly iron sulfide oxidation, could be operating in the upper lake and fish farms (reaction 6). The high values of TDS in these waters are mainly due to evaporation, which raises the concentration of all water chemical components.

The lower lake is a closed lake where the annual evaporation is extremely high and exceeds the inflow. The water in this lake is salty, which could be due to either evaporation, saline inflow, or both [39]. Because the lake has no outlet, and the climatic conditions are typically arid throughout most of the year, the lake water gradually evaporates and its salinity increases. The lower lake is recharged by waters of SO_4 equivalent concentration of approximately 14.6 from the upper lake; this water is subjected to intensive evaporation that increases the SO_4 equivalent to approximately 50 meq/l. The anionic concentration follows the same order as in the upper lake ($Cl > SO_4 > HCO_3$); however, the average TDS increases from approximately 2658 mg/l in the upper lake to approximately 14963 mg/l in the lower lake. Fig. 6e shows that the correlation between SO_4 and Ca is not significant ($R^2 = 0.4$) with respect to the waters of the upper and lower lakes, except for four (grouped) samples taken from the lower lake. These four samples (samples 3, 7, 9 and 12, Table 1) are characterized by a higher BOD compared to the remaining lower lake samples. This means that biological processes, especially fish respiration,

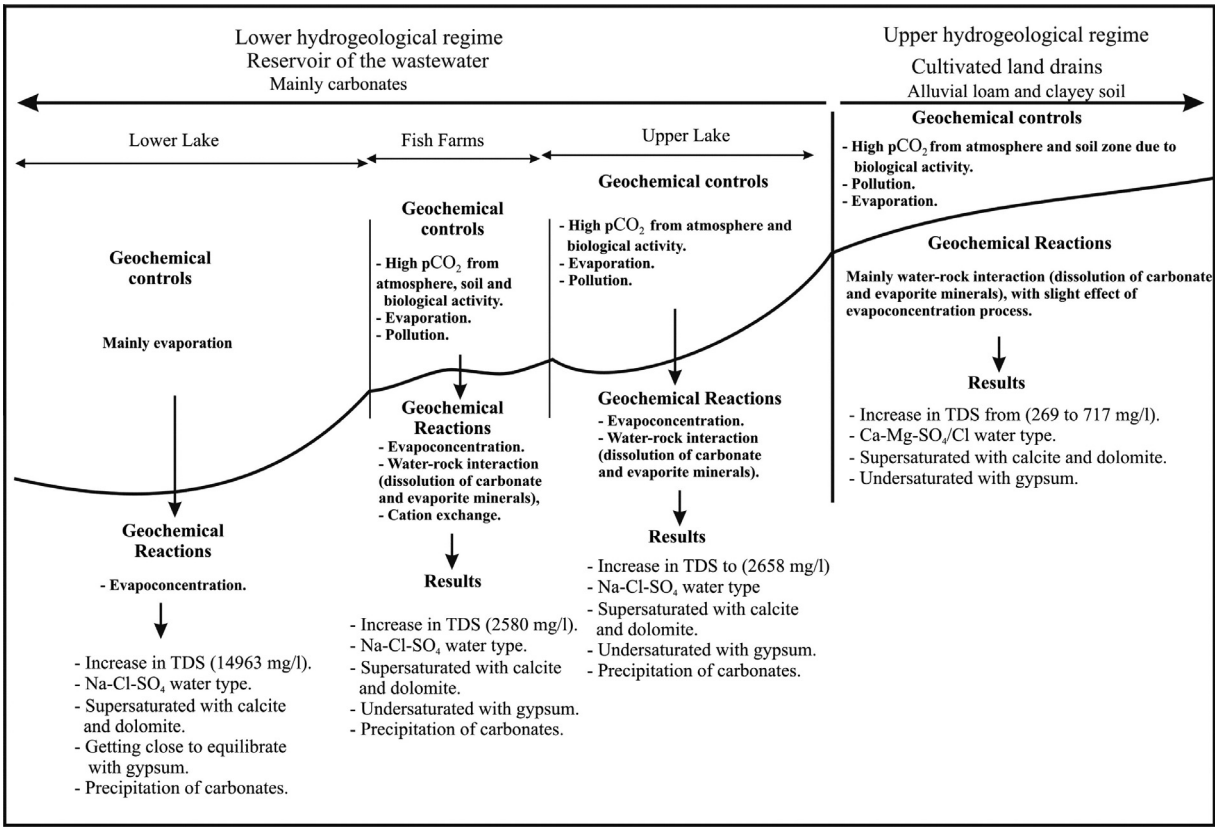

Fig. 9 Schematic cross section showing the suggested evolution path of the drainage water in the area.

increase the concentration of dissolved CO_2 in the water that leads to an increase of the carbonate dissolution, which in turn raises the concentration of Ca (reaction 5, Fig. 6). The increase in Ca concentration decreases the Mg/Ca equivalent ratio (Fig. 6d), which means that cation exchange (reactions 4a, c) could contribute to the increasing Ca concentration in these four samples (Fig. 6g and h). As SO_4 behaves conservatively during evaporation while the water is still undersaturated with respect to gypsum, the shift of these four water samples is completely due to chemical reactions that increase Ca that could be from the dissolution of both carbonates and gypsum (Fig. 6e, g, h).

To explain the elevated sulfate concentration, it is likely that gypsum dissolution has occurred in the bedrock. In agreement with [40], the coexistence of Na^+, Cl^- and SO_4^{2-} can be explained by the presence of evaporites in the study area. Gypsum is abundant in the Faiyum area [41,42]. Additionally, gypsum is added to improve Faiyum's soil productivity [43]. In addition, the current status of the soil salinity, sodicity, and water table indicates that most lacustrine and alluvial-lacustrine soils in the Faiyum Depression are actually degraded by salinization, sodification and waterlogging [44]. All of the drainage water samples lie in regions of lacustrine and alluvial-lacustrine soils that are rich in gypsum and soil salts. As a result, congruent dissolution of soluble minerals such as gypsum ($CaSO_4{\cdot}2H_2O$) and halite (NaCl) from these types of soils leads to very high ion concentrations. The SI of gypsum for all of the study water samples (Fig. 8c) shows that under-saturation with respect to gypsum is prevalent in the area. Therefore, dissolution of gypsum and halite is expected to contribute to the solute budget as water flows toward the depression lakes.

From the preceding discussion, two hydrogeochemical regimes can be distinguished in the region (Fig. 9). The upper hydrogeological regime, which is represented by the cultivated land, is rich in soils, alluvium loam, clays and evaporites. This land has been irrigated mainly from dense irrigation canals branching out of Bahr Youssef. The cultivated land drainage is finally collected in one drainage channel (El Wadi Drain), which carries the cultivated land wastewater to the Wadi El Raiyan depression lakes; the lower hydrogeological regime (Fig. 9) is an artificial surface reservoir of the wastewater.

Conclusions

1. The main freshwater source in the study area is Nile water via the Bahr Youssef channel. The TDS of this water is approximately 269 mg/l. The cationic composition follows the order Ca > Na > Mg > K (in equivalents), while the anionic composition is in the order HCO_3 > Cl/SO_4, which is similar to the common natural water ion assemblages established for world rivers, Ca > Mg > Na > K and HCO_3 > SO_4 > Cl. The water is slightly alkaline (pH = 7.8), and its water type is Ca–Mg–HCO_3 (T1). The irrigation water is undersaturated with respect to calcite, dolomite and gypsum minerals.
2. The study area can be subdivided into two hydrogeological regimes according to variation in bedrock geology, elevation

and other factors and activities that control geochemical reactions.

3. The dissolution of carbonate and evaporite minerals in addition to cultivation, anthropogenic sources of pollution, and evaporation increase the average TDS to approximately 717 mg/l in the cultivated land drainage. Na and Cl ions increase in these waters due to dissolution of halite and pollution, leading to a change in the cationic and anionic order to follow Na > Ca > Mg > K and Cl > HCO_3 > SO_4. The water type developed to Na-SO_4/Cl (T2), which tends to be predominantly influenced by the chemical weathering of rocks and minerals. The water becomes saturated to supersaturated with carbonate minerals.
4. El Wadi Drain discharges its drainage water to the upper lake. The lake has been formed in carbonate rocks. The drainage water is detained in this lake before reaching the lower lake. Evapoconcentration and water–rock interaction enhance the average TDS to become 2658 mg/l.

The water becomes alkaline (pH = 8.5). The ionic constituents of the water follow the same order as that in the cultivated drainage except that the SO_4 concentration exceeds the HCO_3 concentration. This could be accompanied by the precipitation of carbonate minerals as the water becomes completely supersaturated with respect to calcite and dolomite. The water type becomes completely Na–Cl–SO_4 (T2).

5. The area of fish farms is located between the upper and lower lakes and is mainly recharged from the upper lake water. This area is also surrounded by wild and cultivated lands on a plausible soil thickness rich in clays. The factors controlling the chemical composition of the drainage water in this area are quite similar to those in the upper lake. The final additional factor is the cation exchange process that seems to be active due to the availability of clays in soils that are in contact with water rich in Na. This leads to increases in the Ca concentration in the water and precipitation of carbonate minerals.
6. In the lower lake at the last station, the drainage water has been detained for a long period. The only way to escape is through evaporation. The evapoconcentration process with selective precipitation of some minerals mainly prevails and controls the chemical composition of the drainage water, being alkaline (pH = 8.5) with Na-Cl-SO_4 water type. Precipitation of carbonate minerals is commonly expected. The water is going to equilibrate with gypsum.

Conflict of Interest

The authors have declared no conflict of interest.

Compliance with Ethics Requirements

This article does not contain any studies with human or animal subjects.

Acknowledgments

The authors would like to express their appreciation to the team of the central chemical analysis laboratories of the National Water Research Centre, El-Kanater El-Khairia, Egypt, for doing the analysis.

References

[1] El-Shabrawy GM. Ecological studies on macrobenthos of Lake Qarun, El-Fayum, Egypt. J Egypt Acad Soc Environ Dev 2001;2:29–49.
[2] Saleh MA. Ecological investigation of inorganic pollutants in El-Faiyum and El-Raiyan aquatic environment. Supreme Council of Universities, FRCU, Rep; 1985, p. 1–54.
[3] Sayed MF, Abdel-Satar AM. Chemical assessment of Wadi El-Rayan lakes, Egypt. Am-Eurasian J Agric Environ Sci 2009;5(1):53–62.
[4] Mansour SA, Sidky MM. Ecotoxicological Studies. 6. The first comparative study between lake Qarun and Wadi El-Rayan wetland (Egypt), with respect to contamination of their major components. Food Chem 2003;82:181–9.
[5] Abd-Ellah RG. Physical limnology of El-Fayoum depression and their budget. PhD Thesis. Faculty of Science, South Valley University; 1999. 140 pp.
[6] Clark FW. Data of Gechemistry, US Geol Surv. Bull., 5th ed. US Government Printing Office, Washington, DC; 1924. p. 770.
[7] Alekin OA, Brazhnikova LV. Contribution to knowledge of dissolved matter runoff at the earth's surface. Gidrochim Mat 1960;32:12–34.
[8] Alekin OA, Brazhnikova LV. Dissolved matter discharge and mechanical and chemical erosion. Int Assoc Sci Hydrol 1968;78:35–41.
[9] Livingstone DA. Chemical composition of rivers and lakes. Data of Chemistry, USGS prof 1963; Paper 440 G. p. 1–64.
[10] Gibbs RJ. Water chemistry of the Amazon River. Geochim Cosmochim Acta 1972;36:1061–6.
[11] Stallard RF, Edmond JM. Geochemistry of the Amazon: 1. Precipitation chemistry and the marine contribution to the dissolved load at the time of peak discharge. J Geophys Res 1981;86:9844–55.
[12] Stallard RF, Edmond JM. Geochemistry of the Amazon: 2. The influence of geology and weathering environment on the dissolved load. J Geophys Res 1983;88:9671–88.
[13] Stallard RF, Edmond JM. Geochemistry of the Amazon: 3. Weathering chemistry and limits to dissolved inputs. J Geophys Res 1987;92:8293–302.
[14] Sarin MM, Krishnaswami S, Dili K, Somayajulu BLK, Moore WS. Major ion chemistry of the Ganga-Brahmaputra river system: weathering processes and fluxes to the bay of Bebgal. Geochim Cosmochim Acta 1989;53:997–1009.
[15] Sarin MM, Krishnaswami S, Trivedi JR, Sharma KK. Major ion chemistry of the Ganga source waters: weathering in the high altitude Himalaya. Proc Ind Acad Sci (Earth Planet Sci) 1992;101:89–98.
[16] Galy A, France-Lanord C. Weathering processes in the Ganges-Brahmaputra basin and the riverine alkalinity budget. Chem Geol 1999;159:31–60.
[17] Gordeev VV, Sidorov LS. Concentrations of major elements and their outflow into the Laptev Sea by the Lena River. Mar Chem 1993;43:33–45.
[18] Huh Y, Tsoi MY, Zaitsev A, Edmond JM. The fluvial geochemistry of the rivers of eastern Siberia: I. Tributaries of the Lena River draining the sedimentary platform of the Siberian Craton. Geochim Cosmochim Acta 1998;62:1657–76.
[19] Huh Y, Panteleyev G, Babich D, Zaitsev A, Edmond JM. The fluvial geochemistry of the rivers of Eastren Siberia: II. Tributaries of the Lena, Omoloy, Yana, Indigirka/Kolyma, and Anadyr draining the collisional/accretionary zone of the Verkhoyansk and Cherskiy ranges. Geochim Cosmochim Acta 1998;62:2053–75.

[20] Reeder SW, Hitchon B, Levinson AA. Hydrochemistry of the surface waters of the Machenzie River drainage basin, Canada: 1. Factors controlling inorganic composition. Geochim Cosmochim Acta 1972;36:181–92.
[21] Stallard RF, Koehnken L, Johnson MJ. Weathering processes and the composition of inorganic material transported through the Orinoco River system, Venezuela and Colombia. Geoderma 1991;51:133–65.
[22] Edmond JM, Palmer MR, Measures CI, Brown ET, Huh Y. Fluvial geochemistry of the eastern slope of the northeastern Andes and its fore deep in the drainage of the Orinoco in Colombia and Venzuela. Geochim Cosmochim Acta 1996;60: 2949–76.
[23] Saleh MA, Ewane E, Jones J, Wilson BL. Monitoring Wadi El Raiyan Lakes of the Egyptian Desert for Inorganic Pollutants by Ion-Selective Electrodes, Ion Chromatography, and Inductively Coupled Plasma Spectroscopy. Ecotoxicol Environ Saf 2000;45: 310–6.
[24] Saleh Mahmoud A, Saleh Mostafa A, Fouda Mostafa M, Saleh Magdy A, Abdel Lattif Mohamed S, Wilson Bobby L. Inorganic pollution of the Man-Made lakes of Wadi El-Raiyan and its impact on aquaculture and wildlife of the surrounding Egyptian desert. Arch Environ Contain Toxicol 1988;17:391–403.
[25] Said R. The geology of Egypt. Amsterdam: Elsevier; 1962, 377 pp.
[26] Hammad MA, Abo-El-Ennan SM, Abed F. Pedological studies on the Fayoum area, Egypt, landscapes and soil morphology. Egypt J Soil Sci 1983;23(2):99–114.
[27] Said R. The river Nile: geology, hydrology and utilization. Amsterdam: Elsevier; 1993.
[28] Ghabbour TK. Soil salinity mapping and monitoring using remote sensing and a geographical information system (some applications in Egypt). Ph.D. Thesis, Fac of Sci, State University, Ghent; 1988. 195pp.
[29] Shendi MM. Some mineralogical aspects of soil sediments with special reference to both lithology and environmental conditions of formation in Fayoum area, Egypt. Ph.D. Thesis, Fac of Agriculture, El-Fayoum Cairo University, Egypt; 1990. 227 pp.
[30] Abdel Wahed MM, Mohamed EA, El-Sayed MI, M'nif A, Sillanpää M. Geochemical modeling of evaporation process in Lake Qarun, Egypt. J Afr Earth Sci 2014;97:322–30.
[31] Parkhurst DL. User's guide to PHREEQC- a computer program for speciation, reaction-path, advective-transport, and inverse geochemical calculations. Water resources investigations report 95-4227. USGS, Earth Sciences Information Section. Box 25286, MS 517, Denver Federal Centre, Denver, CO80225; 1995. 151p.
[32] Chadha DK. A proposed new diagram for geochemical classification of natural waters and interpretation of chemical data. Hydrogeol J 1999;7:431–9.
[33] Gibbs RJ. Mechanisms controlling world water chemistry. Science 1970;170(3962):1088–90.
[34] Gibbs RJ. Mechanisms controlling world water chemistry: evaporation-crystallization process. Science 1971;172:871–2.
[35] Meybeck M. Concentrations des eaux fluviales en èlèments majeurs et apports en solution aux ocèans. Rev Gèol Dyn Gèoger Phys 1979;21(3):215–46.
[36] Berner EK, Berner RA. Global environment: water, air, and geochemical cycles. Prentice-Hall, Inc.; 1996, p. 376.
[37] Drever JI. The geochemistry of natural waters. third ed. Englewood Cliffs, NJ: Prentice-Hall; 1997, 436 p..
[38] Hounslow AW. Water quality data. Analysis and interpretation. New York: Lewis Publishers; 1995, p. 182.
[39] Eugster HP, Hardie LA. Saline Lakes. In: Lerman A, editor. Lakes: chemistry, geology, physics. New York, NY: Springer; 1978. p. 237–93.
[40] Huang X, Sillanpää M, Gjessing ET, Vogt DR. Water quality in the Tibetan Plateau: major ions and trace elements in the headwaters of four major Asian rivers. Sci Tot Environ 2009;407:6242–54.
[41] Aref MAM. Classification and depositional environments of Quaternary pedogenic gypsum crusts (gypcrete) from east of the Fayum Depression, Egypt. Sediment Geol 2003;155:87–108.
[42] Keatings KW, Hawkes I, Holmes JA, Flower RJ, Leng MJ, Abu-Zied RH, et al. Evaluation of ostracod-based palaeoenvironmental reconstruction with instrumental data from the arid Faiyum Depression, Egypt. J Paleolimnol 2010;38: 261–83.
[43] Abdel Kawy WAM, Belal A. Use of satellite and GIS for soil mapping and monitoring soil productivity of the cultivated land in El-Fayoum Depression, Egypt. Arab J Geosci 2013;6(3): 723–32.
[44] Ali RR, Abdel Kawy WAM. Land degradation risk assessment of El Fayoum Depression, Egypt. Arab J Geosci 2013;6(8): 2767–76.